A Study of Dose Painting with IMRT Guided by Perfusion-weighted Magnetic Resonance Imaging for Brain Metastases

Chuanke Hou
Shandong Cancer Hospital and Institute
Guanzhong Gong
Shandong Cancer Hospital and Institute
Lizhen Wang
Shandong Cancer Hospital and Institute
Ya Su
Shandong Cancer Hospital and Institute
Jie Lu
Shandong Cancer Hospital and Institute
Yong Yin (yinyongsd@126.com)
Shandong Cancer Hospital and Institute

Research

Keywords: Brain metastases, Radiotherapy, Dose escalation, 3D arterial spin labeling, Subvolume

Posted Date: December 22nd, 2020

DOI: https://doi.org/10.21203/rs.3.rs-131837/v1

Abstract

Purpose: To investigate dose escalation for brain metastases (BM) subvolumes with low cerebral blood flow (CBF) using dose-painting technology based on MR 3D arterial spin labeling (3D-ASL) images.

Methods: A total of 50 patients with single BM were selected for this study. CT and MR simulation images, including contrast-enhanced T1-weighted (T1W) images and CBF images, were obtained. The gross tumor volume (GTV) was determined by fusion of contrast-enhanced CT and T1W images, and this volume was divided into high- and low-perfusion areas according to the difference in CBF. Sub-volume with less than 25% of the maximum CBF was defined as hypoxic region GTV_H which was settled for dose escalation. The planning target volume (PTV) and PTV_H were calculated from the GTV and the GTV_H, respectively. The PTV_N was calculated by subtracting the PTV_H from the PTV. Plan 1 was defined as the conventional plan with a prescription dose of 60 Gy for the PTV. Plan 2 and Plan 3, respectively, escalated the prescription dose for the PTV_H to 72 Gy with and without the maximum dose constrained based on Plan 1. Dosimetric indices were compared among the three plans.

Results: On average, the GTV volume was 34.53 cm^3, and the GTV_H volume was 16.95 cm^3, accounting for 49.09% of the GTV. Compared to Plan 1, the $D_{2\%}$, $D_{98\%}$ and D_{mean} values of the PTV_H escalated by 20.50%, 19.32%, and 19.60%, respectively, in Plan 2 and by 24.05%, 6.77%, and 17.00%, respectively, in Plan 3 (all $P<0.05$). The doses administered in Plans 2 and 3 were 73.67±0.34 Gy and 72.37±0.61 Gy, respectively (both $P<0.05$). In Plans 2 and 3, respectively, the conformity index of PTV_H was increased by 45.45% and 63.64%; meanwhile, the homogeneity index was sacrificed, increasing from 0.04 to 0.05 and 0.11 (all $P<0.05$). Plan 2 achieved better values of $D_{98\%}$ and D_{mean}, as well as a smaller increase in the homogeneity index, than Plan 3. The doses received by organs at risk (OARs) did not significantly differ between the conventional plans and the boost plans (all $P>0.05$).

Conclusions: Targeted dose escalation guided by the 3D-ASL-based CBF differences in BM effectively escalated the dose delivered to low-CBF subvolumes without increasing the dose to OARs.

Introduction

Brain metastases (BM) are the most common intracranial malignant tumors, and approximately 8–10% of tumor patients will develop BM during their disease course[1]. At present, the main treatment for BM is radiotherapy (RT), primarily whole brain radiotherapy (WBRT) and stereotactic radiosurgery (SRS)[2, 3]. Although high-dose SRS plays an important role in the treatment of small-volume BM, its clinical application to large-volume BM is limited because of the risk of radiation-induced brain injury[4]. Large-volume BM are more heterogeneous than small ones because of the long growth cycle and complex blood supply of the former; chiefly as a result of this heterogeneity, different regions of large-volume BM respond differentially to RT[5–7]. Previous investigation has demonstrated that large-volume tumors such as neck and head cancers have extensive hypoxic areas and that the volume of hypoxic tissue is closely

related to the tumor volume[8]. It has been widely reported that tumor hypoxia is related to RT resistance and poor prognosis[5–8].

Despite being a common strategy to recognize hypoxic regions, positron emission tomography-computed tomography(PET-CT) has shortcomings such as poor resolution and unclear presentation of tumor boundaries[9–12]. Functional magnetic resonance(MR) can address this problem by simultaneously providing anatomical and histobiological information on tumors; this technique is superior to conventional MR in evaluating the internal microenvironment of solid tumors. Dynamic contrast enhanced (DCE) can obtain hemodynamic parameters such as cerebral blood flow (CBF), cerebral blood volume (CBV) and time-to-peak (TTP), which is the main technique for clinical perfusion of MRI[13]. However, DCE has the disadvantages of inaccurately reflecting the damaged area without blood-brin brrier (BBB), long imaging time and contrast medium injection. Notably, three-dimensional arterial spin labeling (3D-ASL) perfusion imaging, which uses hydrogen protons in blood as a contrast medium, analyzes CBF parameters noninvasively and quantitatively, and tumor perfusion information is reflected indirectly[14, 15]. Theoretically, a subvolume with low CBF is a hypoxic or potentially hypoxic area[5]. Accurate identification of these areas, followed by targeted dose escalation for them, can solve the problem of local RT resistance and improve the curative effect of treatment[16].

Safe targeted dose escalation for the low-CBF subvolumes of BM will help to improve local control and patient prognosis of patients on the basis of compared to population dose division. Therefore, this study examines the feasibility and dosimetric characteristics of subvolume segmentation and dose escalation for BM based on the intratumoral distribution of CBF.

Materials And Methods

Patients

From July 2018 to April 2020, 50 patients with single BM who received only RT were selected, including 29 males (age range: 33–74 years old; average age: 58.24 years old) and 21 females (age range: 34–72 years old; average age: 55.76 years old). There were 33 cases secondary to lung cancer, 9 cases secondary to breast cancer, 4 cases secondary to renal carcinoma, 2 cases secondary to esophageal cancer and 2 cases secondary to colon cancer. The patient eligibility criteria were as follows: an imaging-based diagnosis of BM; no contraindications to CT or MR; clear images with no artifacts; and a maximum tumor cross-sectional diameter of more than 2 cm.

This study was approved by the Medical Ethics Approval Committee at Shandong Cancer Hospital and Institute. The need for informed consent was waived by the Medical Ethics Committee because the study was an observational, retrospective study using a database from which the patients' identifying information had been removed.

Computed tomography (CT) and MR simulation

CT simulation images with a slice thickness of 3 mm and an interslice gap width of 3 mm were obtained with a CT scanner (Brilliance Big Bore, Philips, Netherlands). MR imaging was performed on a 3.0 T superconducting MR scanner (Discovery 750W, GE Healthcare, USA) if the head position was the same as in the CT simulation. 3D-ASL and contrast-enhanced T1-weighted (T1W) image data were acquired using 3D volume scanning with a 26 cm field of view (FOV), a matrix size of 256 × 256, and a slice thickness of 3 mm. For 3D-ASL, the special acquisition conditions were as follows: repetition time (TR), 5160 ms; echo time (TE), 11.5 ms; postlabel delay, 2025 ms. For contrast-enhanced T1W images, a TR of 8.5 ms and a TE of 3.2 ms were used. Gadopentetate dimeglumine was power-injected at doses standardized by patient body weight (0.2 mL/kg body weight) at 2 mL/s, and the scan was started after 3–5 min after injection.

Target volume definition

Contrast-enhanced CT and T1W images were fused and registered in MIM Maestro software (6.8.8, USA), and the gross tumor volume (GTV) was defined as the region with high signal and obvious enhancement on MR. On this basis, different targeted subvolumes within the BM were identified according to their different CBF values, as follows.

The hypoperfused subvolume GTV_H was defined as the region with less than 25% of the maximum CBF, serving as the target subvolume for dose escalation[17]. The high-perfusion subvolume was defined as the region with at least 25% of the maximum CBF. The nonperfused subvolume was defined as the region with low signal on contrast-enhanced T1W images and nonperfusion on CBF images. The high-perfusion and nonperfusion subvolumes together were considered the normal prescription dose region GTV_N. The planning target volume (PTV) was designed to allow a 5 mm margin beyond the GTV, and a 3 mm margin was added to the GTV_H to obtain the PTV_H. And the PTV_N was calculated by subtracting the PTV_H from the PTV, and the small volume that could not be identified was classified as part of the PTV_N. A schematic diagram is shown in Fig. 1.

Treatment planning

Conventional and simultaneous integrated boost (SIB) intensity-modulated radiotherapy (IMRT) plans were defined using Eclipse (Version 15.6, Varian, USA) for the PTV and PTV_H, respectively. The conventional plan, designated Plan 1, prescribed 60 Gy to the primary PTV with a maximum dose constraint of 66 Gy. Plan 2 was based on Plan 1 but included a boost of 12 Gy to the GTV_H with a maximum dose constraint of 79 Gy. The settings of Plan 3 were the same as those of Plan 2 except that no maximum dose constraint was applied to the PTV_H.

The optimized parameters and dose constraints for organs at risk (OARs) in the three plans were unified. OARs were restricted to the following doses: maximum dose (D_{max}) < 50 Gy for each eye, D_{max}<54 Gy for each optic nerve, D_{max} < 8 Gy for each lens, and D_{max} <54 Gy for the brainstem.

Dose calculation was performed in anisotropic analytical algorithm optimization mode (version 15.512) using 6 MV X-rays. The calculated grid was 2.5 mm × 2.5 mm, and the prescription covered 95% of the target volume.

5. Plan evaluation

In order to compare the three treatment plans, the dose distribution and dose-volume histograms (DVHs) of the PTV, PTV_H, PTV_N and OARs were calculated. Thus, the $D_{2\%}$, $D_{98\%}$, and D_{mean} of the PTV were counted. The D_{max} values of the bilateral eyeballs, bilateral optic nerves, bilateral lenses and brainstem were compared. Furthermore, the target coverage, conformity index (CI) and homogeneity index (HI) were calculated. A CI near 1 indicates that region receiving the reference dose closely matches the shape of the target region, and an HI close to 0 indicates good uniformity[18]. The formulas for calculating CI and HI are as follows:

$$\mathrm{CI} = \frac{V_{t,ref}}{V_t} \times \frac{V_{t,ref}}{V_{ref}}; \quad \mathrm{HI} = \frac{D_{2\%} - D_{98\%}}{D_{\mathrm{Prescription}}}$$

where V_t represents the volume of the target region, $V_{t,ref}$ represents the volume of the target region covered by the reference dose, and V_{ref} represents the volume of all region covered by the reference dose.

A flowchart of this study is shown in Fig. 2.

Statistics

Statistical analysis was performed using IBM SPSS Statistics Version 22.0. Analysis of variance was used to evaluate the differences among the three plans. The least significant difference (LSD) was used in pairwise comparisons. All data are expressed as $\bar{x} \pm s$ (mean ± standard deviation), and $P < 0.05$ indicates a significant difference.

Results

Target volume

On average, the GTV was 34.53 cm^3, and the GTV_H was 16.95 cm^3, accounting for 49.09% of the GTV. The average PTV, PTV_H and PTV_N were 71.97 cm^3, 41.46 cm^3 and 30.51 cm^3, respectively. The ratios of PTV_H to PTV and PTV_N to PTV were 57.61% and 42.39%, respectively, as shown in Table 1 and Fig. 3.

Table 1
Volume and volume ratio of each target area in all patients

Target area	Volume(cm^3)	Volume ratio(%)
GTV	34.53 ± 21.73	—
GTV_H	16.95 ± 11.89	49.09
PTV	71.97 ± 34.68	—
PTV_H	41.46 ± 22.03	57.61
PTV_N	30.51 ± 18.55	42.39

Dosimetric comparison

Compared with Plan 1, the $D_{2\%}$, $D_{98\%}$ and D_{mean} of the PTV were increased by 20.18%, 8.34% and 18.38%, respectively, in Plan 2 and by 24.05%, 6.77% and 17.00%, respective, in Plan 3. Regarding the PTV_H, the $D_{2\%}$, $D_{98\%}$ and D_{mean} of Plan 2 were increased by 20.50%, 19.32% and 19.60%, respectively, while those of Plan 3 were increased by 24.05%, 6.77% and 17.00%, respectively. Additionally, the $D_{2\%}$, $D_{98\%}$ and D_{mean} of the PTV_N were improved in Plans 2 and 3 as follows: 18.81%, 7.17%, and 14.31% and 19.69%, 5.15%, and 11.80%, respectively.

There was no significant difference in the $D_{2\%}$ of the PTV_N between Plans 2 and 3 ($P > 0.05$), but the differences in the other parameters were statistically significant ($P < 0.05$). Notably, the $D_{2\%}$ values of the PTV, PTV_H and PTV_N all showed increasing trends among the three plans, while the improvement rates of the $D_{98\%}$ and D_{mean} were higher for Plan 2 than for Plan 3, as shown in Table 2 and Fig. 4.

Table 2
Comparison of D2%、D98% and Dmean among three plans

Program		Plan1	Plan2	Plan3	*F*	*P*	P_1	P_2	P_3
PTV	$D_{2\%}$(Gy)	64.42 ± 0.37	77.42 ± 0.62	79.91 ± 2.28	1818.024	0.000	0.000	0.000	0.000
	$D_{98\%}$(Gy)	61.17 ± 0.66	66.27 ± 2.07	65.31 ± 2.25	112.920	0.000	0.000	0.000	0.009
	D_{mean}(Gy)	63.29 ± 0.19	74.92 ± 0.68	74.05 ± 0.84	5178.923	0.000	0.000	0.000	0.000
PTV_H	$D_{2\%}$(Gy)	64.38 ± 0.61	77.58 ± 0.52	80.40 ± 2.39	1727.402	0.000	0.000	0.000	0.000
	$D_{98\%}$(Gy)	61.74 ± 0.69	73.67 ± 0.34	72.37 ± 0.61	6660.500	0.000	0.000	0.000	0.000
	D_{mean}(Gy)	63.43 ± 0.19	75.86 ± 0.08	75.62 ± 0.29	58745.045	0.000	0.000	0.000	0.000
PTV_N	$D_{2\%}$(Gy)	64.39 ± 0.50	76.5 ± 1.19	77.07 ± 2.61	904.842	0.000	0.000	0.000	0.096
	$D_{98\%}$(Gy)	60.55 ± 1.54	64.89 ± 1.83	63.67 ± 1.94	79.330	0.000	0.026	0.000	0.001
	D_{mean}(Gy)	63.05 ± 0.27	72.07 ± 0.71	70.49 ± 0.88	2551.806	0.000	0.000	0.000	0.000

F and *P* were the results of analysis of variance;P_1: Plan1 vs Plan2; P_2: Plan1 vs Plan3; P_3: Plan2 vs Plan3;

The D_{max} received by OARs did not significantly differ between the conventional plan and the boost plans ($P > 0.05$). Nevertheless, the boost plans slightly increased the D_{max} of all OARs compared with Plan 1, with the D_{max} value of the right eye increased by 5.27% to only 0.47 Gy, while those of the other OARs increased by less than 4.10% (2.19%-4.08%), as shown in Table 3.

Table 3
Comparison of organs at risk among three plans

Program	Eye-L (Dmax-Gy)	Eye-R(Dmax-Gy)	Optic nerve-L(Dmax-Gy)	Optic nerve-R(Dmax-Gy)	Lens-L(Dmax-Gy)	Lens-R(Dmax-Gy)	Brainstem(Dmax-Gy)
Plan1	8.74 ± 9.06	8.92 ± 9.99	8.36 ± 12.02	7.36 ± 9.39	2.31 ± 1.54	2.07 ± 1.54	18.68 ± 12.97
Plan2	8.97 ± 8.97	9.39 ± 10.19	8.62 ± 12.21	7.66 ± 9.77	2.37 ± 1.59	2.14 ± 1.55	19.09 ± 13.23
Plan3	8.98 ± 8.75	9.42 ± 10.15	8.67 ± 12.29	7.75 ± 9.83	2.40 ± 1.68	2.15 ± 1.53	19.14 ± 13.30
F	0.012	0.039	0.009	0.023	0.038	0.049	0.018
P	0.988	0.962	0.991	0.978	0.963	0.952	0.982
P1	0.896	0.816	0.916	0.875	0.857	0.805	0.877
P2	0.891	0.804	0.901	0.840	0.787	0.773	0.864
P3	0.995	0.988	0.985	0.965	0.929	0.966	0.987
F and *P* werw the results of analysis of variance;*P1*: Plan1 vs Plan2; *P2*: Plan1 vs Plan3; *P3:* Plan2 vs Plan3;							

Target coverage, CI and HI comparisons

As shown in Table 4, both conventional plans and boost plans achieved 98% target coverage, and Plan 2 achieved PTV_H coverage of up to 99.90%. As for CI, Plan 2 and 3 significantly increased PTV_H CI levels by 45.45% and 63.64%, respectively, compared with Plan 1 ($P < 0.05$). Owing to the use of targeted gradient doses instead of a group-based uniform dose, CI values of the PTV and PTV_N were lower in the boost plans than in the conventional plans. However, a statistically significant difference was found for HI: for all target volumes, Plan 2 outperformed Plan 3, increasing the HI of the PTV_H only slightly (from 0.04 to 0.05).

Table 4
Comparison of target coverage, CI and HI among three plans

Program		Plan1	Plan2	Plan3	*F*	*P*	P_1	P_2	P_3
Target coverage	PTV	99.60 ± 0.60	99.95 ± 0.13	99.86 ± 0.26	10.995	0.000	0.000	0.001	0.211
	PTV_H	99.10 ± 5.19	99.90 ± 0.18	98.40 ± 1.47	2.895	0.058	0.202	0.263	0.017
	PTV_N	99.15 ± 1.41	99.88 ± 0.34	99.76 ± 0.40	10.346	0.000	0.000	0.001	0.488
CI	PTV	0.75 ± 0.07	0.54 ± 0.07	0.55 ± 0.07	144.791	0.000	0.000	0.000	0.244
	PTV_H	0.44 ± 0.10	0.64 ± 0.14	0.72 ± 0.11	78.818	0.000	0.000	0.000	0.000
	PTV_N	0.28 ± 0.09	0.21 ± 0.07	0.21 ± 0.07	12.457	0.000	0.000	0.000	0.814
HI	PTV	0.05 ± 0.01	0.15 ± 0.03	0.20 ± 0.05	258.789	0.000	0.000	0.000	0.000
	PTV_H	0.04 ± 0.02	0.05 ± 0.01	0.11 ± 0.04	101.722	0.000	0.026	0.000	0.000
	PTV_N	0.06 ± 0.03	0.16 ± 0.03	0.19 ± 0.05	167.502	0.000	0.000	0.000	0.000

F and P were the results of analysis of variance; P_1: Plan1 vs Plan2; P_2: Plan1 vs Plan3; P_3: Plan2 vs Plan3;

Discussion

This study demonstrates that, through increased doses to hypoxic or potentially hypoxic low-CBF subvolumes, dose painting with 3D-ASL-defined subvolumes can feasibly be accomplished without increasing the dose delivered to the OARs. This technique holds the potential to achieve better control of BM than can be achieved with traditional RT.

BM is a significant health problem whose incidence is increasing, and the median survival time is only 1–2 months without treatment[1,19–21]. Numerous studies have indicated that increasing the dose of RT significantly improves the local control of BM, and some patients have achieved long-term survival [22, 23]. Therefore, RT is an irreplaceable treatment for BM[3, 4, 22, 23]. However, an increased radiation dose, particularly to vascular endothelial cells and glial cells, is associated with increased toxicity and reduced tolerance to treatment[24]. Thus, dose escalation without guidance is associated with a high risk of radiation damage to brain tissue. Targeted dose escalation in specific locations at risk for radiation

resistance can effective improve on the safety of RT. BM is highly heterogeneous tumors whose radiation-resistant regions consist mainly of hypoxic or potentially hypoxic tissue.

Some studies have shown that BM has highly heterogeneous biological characteristics according to their pathological sources or even their sites of pathological origin[25]. Hypoxia is one of the most important aspects of tumor heterogeneity.

The blood flow in hypoxic tissue is slower than that in normal tissue and cannot satisfy the oxygen requirement of the rapidly proliferating tumor cells because of highly irregular tumor vessels, arteriovenous shunts, blind ends, an incomplete basement membrane of vascular epithelial cells and other factors[26]. Hence, due to the uneven distribution of blood flow and cancer cells, BM tumors appear as RT-sensitive regions with high perfusion, hypoxia radiation-resistant regions with low perfusion, and necrotic regions. Furthermore, the isoeffective dose can be up to three times higher under hypoxic conditions than under normoxic conditions[27]. However, the group-based uniform dose given under a conventional plan cannot guarantee a sufficient dose for radiation-resistant regions, which eventually leads to further tumor progression and recurrence; local control failures are not uncommon under conventional treatment. Accurate and comprehensive identification of hypoxic regions is crucial.

Perfusion-weighted MR can be used for quantitative analysis of blood flow parameters, which is useful for identifying hypoxic regions[14, 15, 17, 28]. The noninvasive technology of 3D-ASL reflects angiogenesis and other functional features of the tumor microvascular system, rather than reflecting only morphology as CT and conventional MR; 3D-ASL provides quantitative information for the diagnosis and treatment of brain tumors from the perspectives of morphology and function [14]. Yukie et al. demonstrated that the area under the curve (AUC) value of ASL for the recognition of hypoxic areas reached 0.830 based on the hypoxia tracer ^{18}F-fluoromisonidazole[10]. Our previous studies also demonstrated that the CBF variations of brain tissue and BM following radiation dose gradients could be quantified by 3D-ASL. With the development of IMRT, a dose escalation method called SIB can implement dose escalation for specific tumor subvolumes[29]. Dose painting aims to apply relatively high radiation doses to hypoxic, radiation-resistant regions to improve tumor control without damaging OARs, and both 3D-ASL and SIB-IMRT are feasible methods for dose painting[30]. Thus, in the present study, SIB-IMRT was used to achieve dose escalation in hypoxic subvolumes that were recognized and segmented by 3D-ASL.

Tumors tend to grow rapidly, showing a hypoxic state of low blood flow, if the growth rate of tumor cells exceeds the production rate of intratumoral blood vessels[25]. Interestingly, 49.09% of the GTV was within a region of low blood flow. Our results showed that an extensive hypoxic subvolume existed within BM and that a dose-painting approach using 3D-ASL is feasible for BM treatment.

Dose painting for hypoxic regions based on various PET tracers has been widely studied in head and neck tumors, but the application of PET is indisputably limited at present because of its invasiveness and high price[11, 12]. In the present study, the results of dose escalation based on 3D-ASL demonstrated that the two boost plans significantly increased the dosimetric indices compared with the conventional plan

of 60 Gy. However, there were two trends. On the one hand, the maximum doses of the three classes of PTVs all took on ascend trend among the conventional plan, the constrained boost plan and the unrestricted one. On the other hand, the constrained boost plan had better average and minimum doses than the other two plans, and this was the case for all three classes of PTVs. Thorwarth et al. noted that doses of up to 82 Gy may be applied to head and neck tumors without increasing toxicity, but constraints for normal tissue were not stated in their work[31].

Our results indicated that the dose delivered to OARs was increased less than 4.10% (2.19%-4.08%) except for the right eye (5.27%; 0.47 Gy) when the prescription dose for hypoxic subvolumes was increased by 20%. Undoubtedly, the absolute dose was still far below the dose constraint. In addition, the constrained boost plan outperformed the unconstrained plan in terms of OAR protection.

The conventional plan and both boost plans achieved target coverage of more than 98%, which indicated that the boost plans met the clinical dose requirement. Likewise, the constrained boost plan had better target coverage than the unconstrained boost plan and the conventional plan. Reducing the uniformity of the radiation dose is beneficial for dose escalation and OAR protection[11]. The HI of the PTV_H increased from 0.04 to 0.05 in Plan 2, suggesting that this boost plan achieved a well-targeted dose distribution. Meanwhile, it is necessary to confirm CI because the shape of the hypoxic subvolume as defined by blood flow is often irregular[30]. In this work, the CI of the hypoxic subvolume was effectively improved through the boost plans with a minor sacrifice in terms of the HI, which further demonstrated the feasibility of our experimental method.

This study demonstrated that hypoxic subvolume delineation and dose escalation based on low CBF are potentially feasible and useful. There are still some limitations in this study. First, post-labeling delay(PLD) is one of the important parameters for accurate evaluation of CBF. However, in practice, it is difficult to ensure that PLD is set according to the specific conditions of patients to adapt to the arrival time of labeled arterial blood. Second, the effect of boost plans for BM still needs to be confirmed in clinical practice. Relevant research is under way.

In summary, hypoxia is one of the main reasons for the poor effect of RT on BM. It is feasible to delineate hypoxic subvolumes and escalate their radiation doses under the guidance of CBF distribution based on the quantitative method of 3D-ASL. An increased dose is targeted to the hypoxic subvolume without increasing the dose delivered to OARs. This approach provides an effective individualized dose-painting strategy for patients with BM.

Abbreviations

BM: Brain metastases; RT: Radiotherapy; SRS: Stereotactic radiosurgery; WBRT: Whole brain radiotherapy; MR: Magnetic resonance; DCE: Dynamic contrast enhancement; CBF: Cerebral blood flow; CBV: Cerebral blood volume; TTP: Time-to-peak; BBB: Blood-brin brrier; 3D: Three dimensional; ASL: Arterial spin labeling; PET-CT: Positron emission tomography-computed tomography; TR: Repetition time; TE: Echo

time; FOV: Field of view; T1W:T1-weighted; CT: Computed tomography; GTV: Gross tumor volume; PTV: Planning target volume; GTVH: Hypoxic gross tumor volume; GTVN: Normal gross tumor volume; PTVH: Hypoxic planning target volume; PTV_N: Normal planning tumor volume; SIB-IMRT: Imultaneous integrated boost intensity-modulated radiotherapy; OARs: Organs at risk; DVHs: Dose-volume histograms; $D_{2\%}$: Radiation dose that covered 2% of PTV; D_{mean}: Radiation dose that covered 50% of PTV; $D_{98\%}$: Radiation dose that covered 98% of PTV; CI: Conformity index; HI: Homogeneity index; LSD: Least significant difference; PLD: Post-labeling delay;

Declarations

Acknowledgments

We gratefully acknowledge Qingtao Qiu for their support with text proofing.

Authors' Contributions

Yong Yin and Guanzhong Gong conceived and designed the study. Lizhen Wang and Ya Su collected data. Chuanke Hou performed the experiments, made a statistical analysis and wrote the paper. Jie Lu reviewed and edited the manuscript. All authors read and approved the manuscript.

Funding

This work was supported by Key Support Program of Natural Science Foundation of Shandong Province (Grant No. ZR2019LZL017) , the Taishan Scholars Project of Shandong Province (Grant No. ts201712098) and National Key Research and Development Program of China (Grant No. 2017YFC0113202).

Availability of data and materials

The data set used and analyzed during the current study are available from the corresponding author on reasonable request.

Ethical approval and consent to participate

This study was approved by the Medical Ethics Approval Committee at Shandong Cancer Hospital and Institute. The need for informed consent was waived by the Medical Ethics Committee because the study was an observational, retrospective study using a database from which the patients' identifying information had been removed.

Consent for publication

Not applicable.

Competing interests

There is no financial or non-financial competing interest for all authors.

References

1. Chamberlain MC, Baik CS, Gadi VK, Bhatia S, Chow LQ. Systemic therapy of brain metastases: non-small cell lung cancer, breast cancer, and melanoma. Neuro Oncology. 2017;19(1):i1-i24.
2. Xin Y, Guo WW, Yang CS, Cui HJ, Hu KW. Meta-analysis of whole-brain radiotherapy plus temozolomide compared with whole-brain radiotherapy for the treatment of brain metastases from non-small-cell lung cancer. Cancer Med. 2018;7(4):981-90.
3. Hughes RT, Masters AH, McTyre ER, Farris MK, Chung C, Page BR, et al. Initial SRS for Patients With 5 to 15 Brain Metastases: Results of a Multi-Institutional Experience. Int. J. Radiat. Oncol. Biol. Phys. 2019;104: 1091-8.
4. Yamamoto M, Kawabe T, Sato Y, Higuchi Y, Nariai T, Barfod BE, et al. A case-matched study of stereotactic radiosurgery for patients with multiple brain metastases: comparing treatment results for 1-4 vs >/= 5 tumors: clinical article. J Neurosurg. 2013;118:1258-68.
5. Lee CT, Boss MK, Dewhirst MW. Imaging tumor hypoxia to advance radiation oncology. Antioxid Redox Signal. 2014;21:313–37.
6. Dewhirst MW, Cao Y, Moeller B. Cycling hypoxia and free radicals regulate angiogenesis and radiotherapy response. Nat Rev Cancer. 2008;8:425–37.
7. Mahmood F, Hjorth Johannesen H, Geertsen P, Hansen RH. Diffusion MRI outlined viable tumour volume beats GTV in intra-treatment stratification of outcome. Radiother Oncol. 2020; 144: 121-6.
8. Dunst J, Stadler P, Becker A, Lautenschläger C, Pelz T, Hänsgen G, et al. Tumor volume and tumor hypoxia in head and neck cancers. The amount of the hypoxia volume is important. Strahlenther Onkol. 2003; 179: 521-6.
9. Salmon E, Bernard Ir C, Hustinx R. Pitfalls and Limitations of PET/CT in Brain Imaging. Semin Nucl Med. 2015; 45: 541-51.
10. Shimizu Y, Kudo K, Kameda H, Harada T, Fujima N, Toyonaga T, et al. Prediction of Hypoxia in Brain Tumors Using a Multivariate Model Built from MR Imaging and F-Fluorodeoxyglucose Accumulation Data. Magn Reson Med Sci. 2020;19: 227-34.
11. Chang JH, Wada M, Anderson NJ, Lim Joon D, Lee ST, Gong SJ, et al. Hypoxia-targeted radiotherapy dose painting for head and neck cancer using (18)F-FMISO PET: a biological modeling study. Acta Oncol. 2013;52:1723-9.
12. Hendrickson K, Phillips M, Smith W, Peterson L, Krohn K, Rajendran J. Hypoxia imaging with [F-18] FMISO-PET in head and neck cancer: potential for guiding intensity modulated radiation therapy in overcoming hypoxia-induced treatment resistance. Radiother Oncol. 2011; 101:369-75.
13. Xu Z, Zheng S, Pan A, Cheng X, Gao M. A multiparametric analysis based on DCE-MRI to improve the accuracy of parotid tumor discrimination. Eur J Nucl Med Mol Imaging. 2019;46(11):2228-34.

14. Wells JA, Thomas DL, Saga T, Kershaw J, Aoki I. MRI of cerebral micro-vascular flow patterns: A multi-direction diffusion-weighted ASL approach. J Cereb Blood Flow Metab. 2017; 37(6):2076-83.
15. Choi YJ, Kim HS, Jahng GH, Kim SJ, Suh DC. Pseudoprogression in patients with glioblastoma: added value of arterial spin labeling to dynamic susceptibility contrast perfusion MR imaging. Acta Radiol. 2013;54(4):448-54.
16. Borghetti P, Pedretti S, Spiazzi L, Avitabile R, Urpis M, Foscarini F, et al. Whole brain radiotherapy with adjuvant or concomitant boost in brain metastasis: dosimetric comparison between helical and volumetric IMRT technique. Radiat Oncol. 2016;11:59.
17. L Li C, Yan JL, Torheim T, McLean MA, Boonzaier NR, Zou J, et al. Low perfusion compartments in glioblastoma quantified by advanced magnetic resonance imaging and correlated with patient survival. Radiother Oncol. 2019;134:17-24.
18. Paddick I. A simple scoring ratio to index the conformity of radiosurgical treatment plans. Technical note. J. Neurosurg. 2000; null: 219-22.
19. Bray F, Ferlay J, Soerjomataram I, Siegel RL, Torre LA, Jemal A. Global cancer statistics 2018: GLOBOCAN estimates of incidence and mortality worldwide for 36 cancers in 185 countries. CA Cancer J Clin. 2018; 68: 394-424.
20. Eichler A F, Loeffler J S. Multidisciplinary management of brain metases. Oncologist. 2007; 12(7):884-98.
21. Nieder C, Norum J, Stemland JG, Dalhaug A. Resource Utilization in Patients with Brain Metastases Managed with Best Supportive Care, Radiotherapy and/or Surgical Resection: A Markov Analysis. Oncology-Basel. 2010; 78(5-6): 348-55.
22. Rades D, Kieckebusch S, Lohynska R, Veninga T, Stalpers LJ, Dunst J, et al. Reduction of overall treatment time in patients irradiated for more than three brain metastases.Int. J. Radiat. Oncol. Biol. Phys.2007;69: 1509-13.
23. Zhuang QY, Li JL, Lin FF, Lin XJ, -Lin H, -Wang Y, et al. High Biologically Effective Dose Radiotherapy for Brain Metastases May Improve Survival and Decrease Risk for Local Relapse Among Patients With Small-Cell Lung Cancer: A Propensity-Matching Analysis. Cancer Control. 2020;27: 1073274820936287.
24. Robbins ME, Brunso-Bechtold JK, Peiffffer AM, Tsien CI, Bailey JE, Marks LB. Imaging radiation-induced normal tissue injury. Radiat Res. 2012;177(4):449-66.
25. Fidler IJ. The Biology of Brain Metastasis: Challenges for Therapy. Cancer J. 2015;21(4):284-93.
26. Brown J M, Giaccia A J. The unique physiology of solid tumors: opportunities (and problems) for cancer therapy. Cancer Res. 1998;58: 1408-16.
27. Eric J Hall, Amato J Giaccia. Radiobiology for the Radiologist[M].2011
28. Colliez F, Fruytier AC, Magat J, Neveu MA, Cani PD, Gallez B, et al. Monitoring combretastatin A4-induced tumor hypoxia and hemodynamic changes using endogenous MR contrast and DCE-MRI. Magn Reson Med. 2016; 75:866-72.

29. van Elmpt W, De Ruysscher D, van der Salm A, Lakeman A, van der Stoep J, Emans D, et al. The PET-boost randomised phase II dose-escalation trial in non-small cell lung cancer. Radiother Oncol. 2012; 104: 67-71.
30. Skjøtskift T, Evensen ME, Furre T, Moan JM, Amdal CD, Bogsrud TV, et al. Dose painting for re-irradiation of head and neck cancer. Acta Oncol. 2018; 57: 1693-9.
31. Thorwarth D, Eschmann SM, Paulsen F, Alber M. Hypoxia dose painting by numbers: a planning study. Int J Radiat Oncol Biol Phys. 2007;68:291-300.

Figures

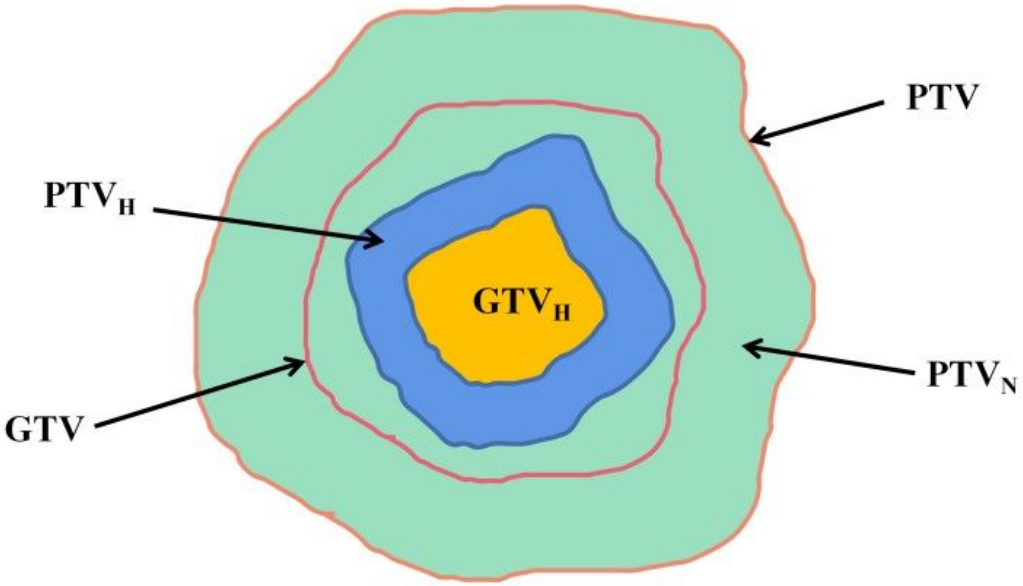

Fig. 1 Illustration of the target volumes: gross target volume (GTV), hypoxia or potential hypoxia sub-volume (GTV_H), GTV extended 5mm to obtain planning target volume(PTV), GTV_H extended 3mm to obtain PTV_H and PTV_N was obtained by subtracting PTV and PTV_H.

Figure 1

Figure 1

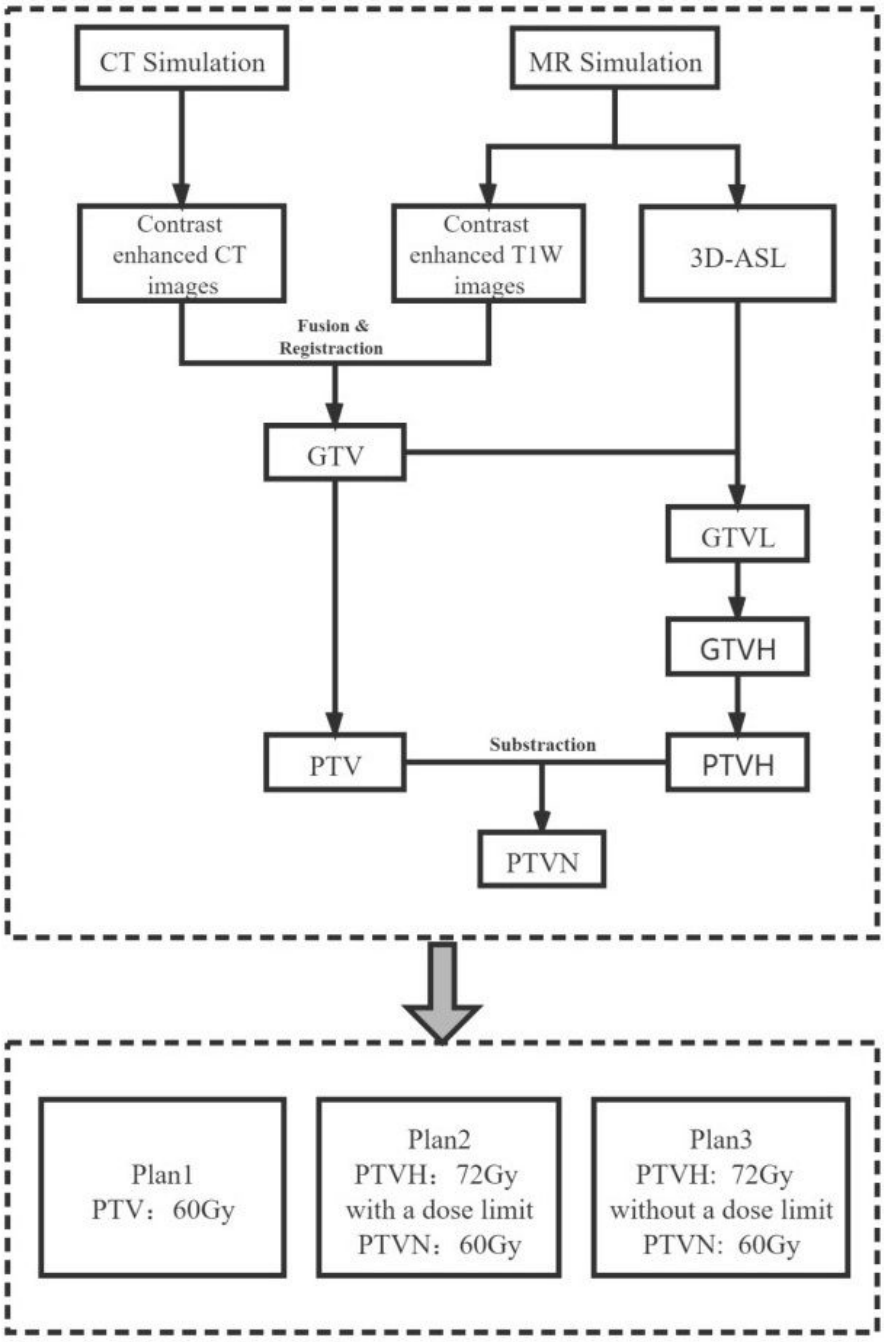

Fig. 2 Working flow chart.

Figure 2

Figure 2

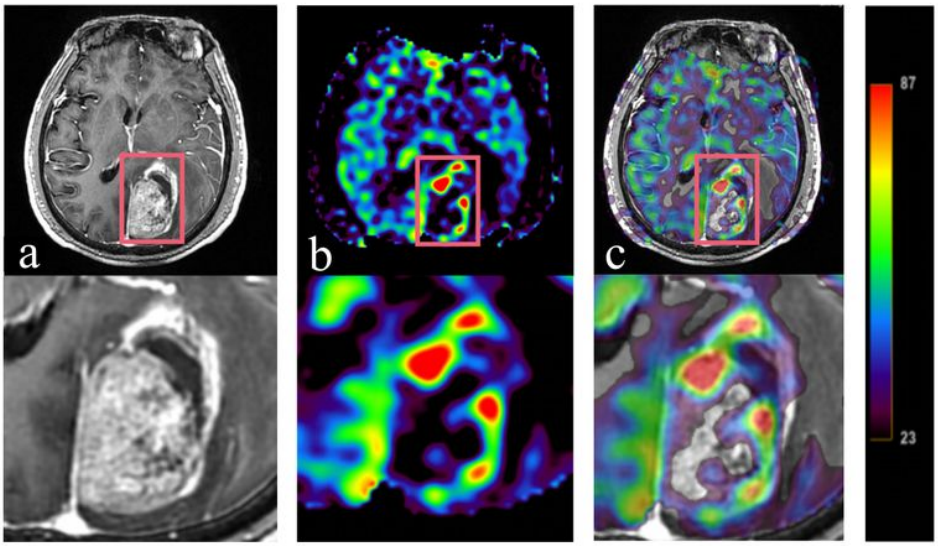

Fig.3 Different tumor information is shown between contrast-enhanced T1W images and 3D-ASL images. A 61 year old male patient diagnosed with brain metastases secondary to colon carcinoma. According to the enhanced area shown in the contrast-enhanced T1W images, 3D-ASL showed the uneven distribution of CBF in tumor. The high cerebral blood flow area is mainly located on the left side of the enhanced edge, while the low area and the enhanced area overlap in a large region. Moreover, the fusion image c shows this result better. a:contrast-enhanced T1W images; b:3D-ASL; c: 3D-ASL fusion registration to contrast-enhanced T1W images.

Figure 3

Figure 3

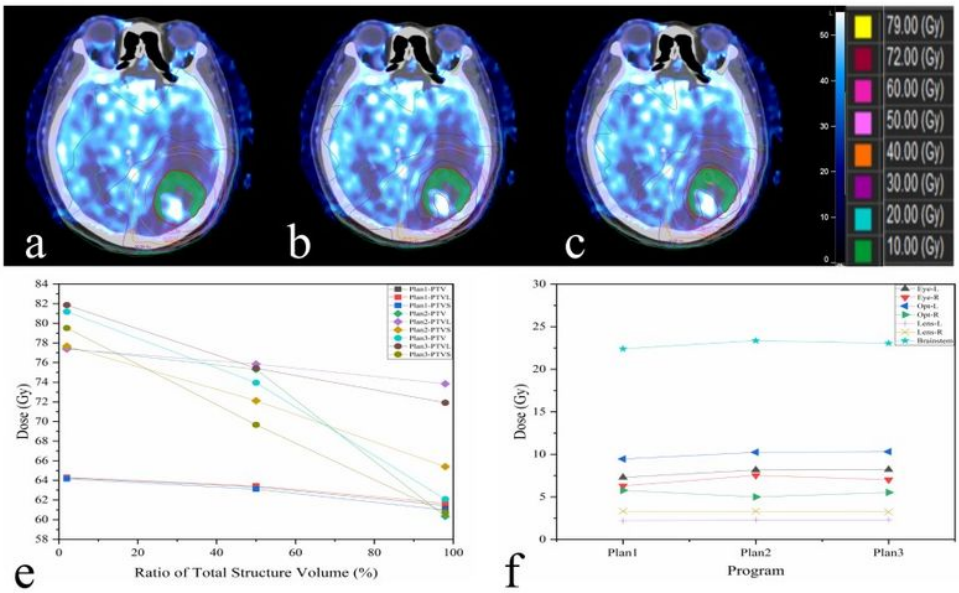

Fig.4 The difference among conventional plan and SIB-IMRT plans are shown in this example(a:Plan1; b:Plan2; c:Plan3;). Display on axial slices for SIB-IMRT plan showing prescribed 72Gy around PTV_H(green).The dosimetric indices $D_{2\%}$, $D_{98\%}$, D_{mean} and the dose received by OARs are also revealed in e and f .

Figure 4

Figure 4